Assessment and Prediction of Land Use/Land Cover Change in the National Capital of Burundi Using Multi-temporary Landsat Data and Cellular Automata-Markov Chain Model

Audace Ntakirutimana and Chaiwiwat Vansarochana*

Faculty of Agriculture, Natural Resource and Environment, Naresuan University, Phitsanulok 65000, Thailand

ARTICLE INFO

Received: 24 Feb 2021
Received in revised: 14 Jun 2021
Accepted: 28 Jun 2021
Published online: 20 Jul 2021
DOI: 10.32526/ennrj/19/202100023

Keywords:
Gitega District/ Land degradation/ Kappa statistics/ Simulation/ Land Change Modeler/ Geoinformatics

*** Corresponding author:**
E-mail: chaiwiwatv@gmail.com

ABSTRACT

Gitega District has experienced significant land use and land cover changes due to human activity. This has increased land degradation and environmental issues. However, there is no data on LULC change to guide land-use planning. This study assessed the rate and magnitude of LULC change over the last 35 years and also simulated future scenarios using Geoinformatics. In the first step, five LULC classes were extracted from satellite images from 1984, 2002, and 2019 using the supervised classification method. Overall accuracy and Kappa statistics of more than 85% and 82% respectively were achieved with 30 reference samples. Change analysis highlighted by Land Change Modeler (1984-2019) indicated a significant increase in Agriculture of 94 km^2, a slight increase in Shrub Land and Built-up Area of 5.5 km^2 and 2 km^2, respectively; and a steep decrease in Trees Cover and Grass Land of 62.5 km^2 and 39 km^2, respectively. Markov Chain and CA-Markov models were further calibrated to simulate LULC changes in 2038 and 2057 using the 2019 base map. Evaluation and analysis of 2019-2057 simulation results showed a moderate agreement of 75% for Kappa and the same trends of LULC change: Trees Cover, Grass Land, and Shrub Land will decrease by 11.5 km^2, 13 km^2, 11.5 km^2 respectively, whereas Agriculture and Built-up Area will increase by 30 km^2 and 6 km^2 respectively in 2057. These study outcomes can support decision-making towards restoration measures of land degradation and long-term environmental conservation in the region.

1. INTRODUCTION

Land cover change denotes alteration in physical land types such as forests, vegetation, and so on, whereas land-use change refers to changes in a specific area of land used or managed by humans for their provisions (Liu and Shi, 2019; Patel et al., 2019). Land use and land cover (LULC) change is a result of the human activities and subsequent development taking place across the world (Bai et al., 2008). Land use pattern is triggered by population dynamics which is directly responsible for the changes in land cover (IPBES, 2018; Serneels and Lambin, 2001; Verma and Raghubanshi, 2019).

The impact of LULC change on the Earth's environment has increased as a result of rapid growth in human population which leads in turn to deforestation, intensive agricultural activities, urbanization, and other unplanned human settlement (Boissière et al., 2009; Lambin et al., 2000; Meyer et al., 1994). According to a global report published by FAO, 24% of the world's land is degraded due to anthropogenic influences, primarily in Africa, Asia, Australia, and North America (Bai et al., 2008). In recent years, assessing and modelling LULC change has become an essential aspect since the LULC change has influences on socioeconomic, and environmental structure (Halmy et al., 2015; Twisa and Buchroithner, 2019).

The study of assessing and modelling LULC change is an expensive and time-consuming process. However, through Remote Sensing (RS) and Geographic Information System (GIS) techniques, it is possible to examine LULC change on large spatial

Citation: Ntakirutimana A, Vansarochana C. Assessment and prediction of land use/land cover change in the National Capital of Burundi using multi-temporary Landsat data and Cellular Automata-Markov Chain Model. Environ. Nat. Resour. J. 2021;19(5):413-426. (https://doi.org/10.32526/ennrj/19/202100023)

and temporal scales (Dewan and Yamaguchi, 2009; Nijimbere et al., 2019). R.S advancements allow us to obtain synoptic information about LULC at a specific time and location (Anderson, 1976; Patil et al., 2012). Multi-temporary satellite images have been widely used for LULC change detection (Kumar et al., 2010; Vila and Barbosa, 2010). The GIS approach, namely Geoinformatics, through its ability to analyze, update and backdate LULC information with object-oriented or pixel-based image classification, has been shown to produce accurate results for LULC monitoring (Mishra et al., 2014; Shen, 2019). Such classification accuracy is performed by both the spatial and spectral resolution of satellite image data (Poursanidis et al., 2015).

Moreover, the future LULC change prediction requires the integration of past trends and current landscape, and plausible assumptions. Therefore, the literature describes various forecasting models based on research purposes, i.e., landscape dynamics, ecological modelling, disaster and deforestation assessment, agriculture projects and urban sprawl planning, etc., (Baker, 1989). Verburg (2006) argues that no single land-use model can be superior to another. But, some other researchers have expressed their confidence in the significant results obtained when integration of Cellular Automata and Markov Chain models is used in the LULC modelling process (Mondal et al., 2016; Nadoushan et al., 2015). Several national land cover mapping programs have been developed to continuously monitor LULC changes and produce national and regional land cover maps (Gómez et al., 2016). This has contributed to a better understanding of natural-human interactions and advanced monitoring and modelling of landscape dynamics (Ghosh et al., 2017; Turner et al., 2007).

Burundi is a small landlocked country with an area of 27,834 km^2, and the most densely populated country in Africa with 480 people/km^2 (UNdata, 2020). Due to an increasing number of householders who rely on agriculture to meet their needs (Moore, 2007), the country is vulnerable to major landscape dynamics and environmental problems (Kamungi et al., 2005; Nzabakenga et al., 2013). It is currently agreed that access to arable land is a top priority for any household. With 90% of the 12 million as workforces in farming land, land resources are being much more depleted and scarcer than in the past (Nzabakenga et al., 2013).

Gitega District, one of the most densely populated regions in Burundi with 476 people/km^2 (Niyuhire, 2018), is prone to land degradation and environmental vulnerabilities as a result of long-term major landscape dynamics. This region has attracted a large number of immigrants due to its geographic location in the center of the country, which is an important aspect of being a National Capital (Guichaoua, 1982). Significant LULC change started occurring in 2007, when the government of Burundi began the process of restoring that district's former status as National Capital (Patel et al., 2019). Thus, the rapid population increase in that area results in agricultural expansion along with built-up area and reduction of forest and grassland in the Gitega's landscape (Guichaoua, 1982; Niyuhire, 2018). As per El-Hassanin et al. (1993) and Marathianou et al. (2000), LULC changes reduce normalized difference vegetation index (NDVI) of land. This provokes other extreme impacts on the environment such as climate change, extreme radiative forcing, pollution and quality reduction of natural ecosystems, changes in hydrological regimes, runoff, soil loss and depletion of soil fertility (IPBES, 2018; Verma and Raghubanshi, 2019). Certain recent studies have only addressed agricultural issues confronting farmers at the national and district levels. Kamungi et al. (2005), land access, Nzabakenga et al. (2013), agriculture and farmers' livelihoods, Nijimbere et al. (2019), soil erosion, Niyuhire (2018), soil depletion and integrated soil fertility. Though, they did not study land degradation with LULC change patterns.

However, Burundi has neither national nor regional mapping platforms for generating basic information about the LULC change and environmental dynamics that could aid in land use planning (Burrell et al., 2018; Ndzabandzaba, 2015). Therefore, the main objective of this study was to assess LULC changes that occurred in the Gitega District over the last 35 year by calculating the rate and magnitude of change for the LULC category. This study also aimed to simulate the future scenario of LULC changes under an assumption of the continuation of past and current trends using the combination of RS, GIS, and Cellular Automata and Markov Chain approach.

2. METHODOLOGY

The Figure 1 shows the overall methodology used for this study in three main parts: data source, data processing, and results analysis.

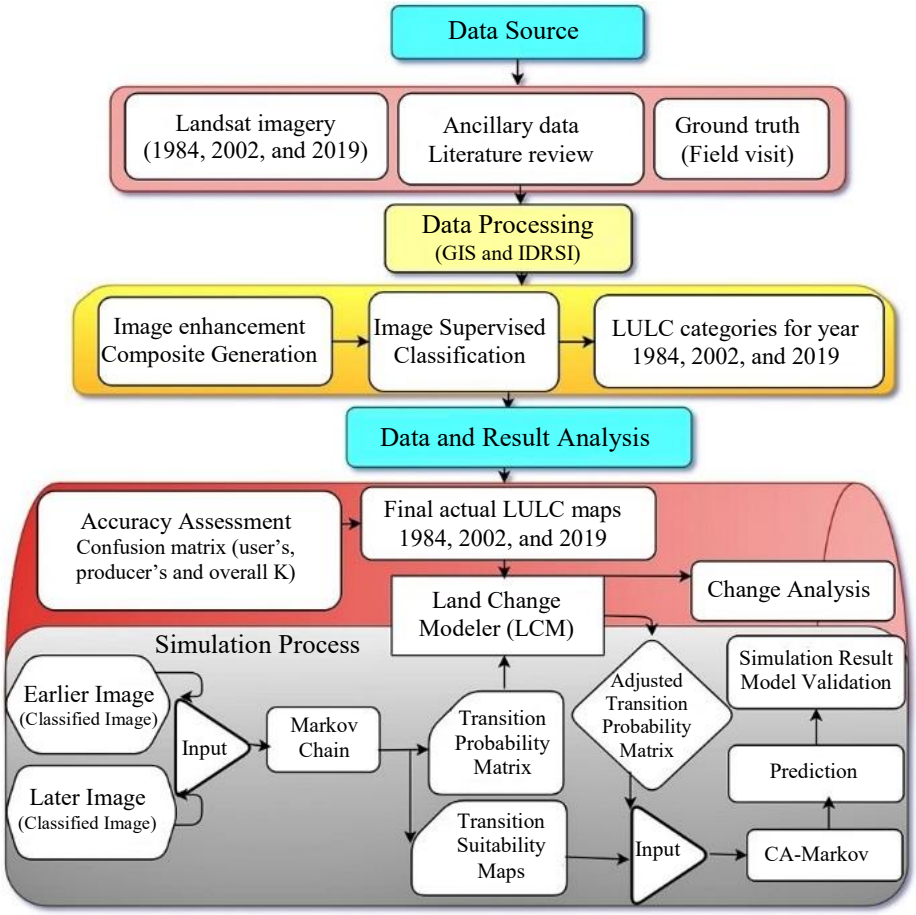

Figure 1. General methodology of the research

2.1 Study area

Gitega District is located in the center of Burundi at a specific geographic grid reference of "03° 25' 35" South Latitude and 29° 50' 37" East Longitude (Figure 2). It has an area of 315 km^2, 150,151 people, and a density of 476 inhabitants/km^2 (Niyuhire, 2018). Its topography dominated by plateau dispersed by hills, valleys, and moderate plains rises between 1,600-2,000 m. Climate is subtropical highland and tropical savanna climate depicting summer and winter (Vassolo et al., 2019). The average annual temperature is 20°C with lower and higher temperatures of 10°C and 26°C respectively, while the average annual rainfall is 1,130 mm with lower and higher rainfall in July and April respectively (Vassolo et al., 2019). Due to those mild climate and plentiful rainfall, the area is ideal for forests, vegetation, and plantations. However, high population pressure on land and poor farming practices are unsuitable for environmental preservation (El-Hassanin et al., 1993; Kamungi et al., 2005). With two harvests per year, cultivation of subsistence foods such as bananas, corn, manioc, sweet potatoes, Irish potatoes, beans, peas, wheat, peanuts, vegetables, etc., is intensified even on steep slopes and hilltops (Kamungi et al., 2005; Nijimbere et al., 2019). This study area, which includes both urban and rural land use characteristics, is likely to experience the most change in its landscape. Since the project to restore its former status as the national capital was launched in 2007, several buildings and road patterns have been constructed to meet the county's second city functions.

2.2 Data acquisition and processing

Three Landsat Images with 30 m resolution were downloaded from the United States Geological Survey (http://earthexpolorer.usgs.gov/) and important information is shown in Table 1. All these images were taken on satellite track path/row:173/062 and projected in UTM with WGS-84 datum 36 N.

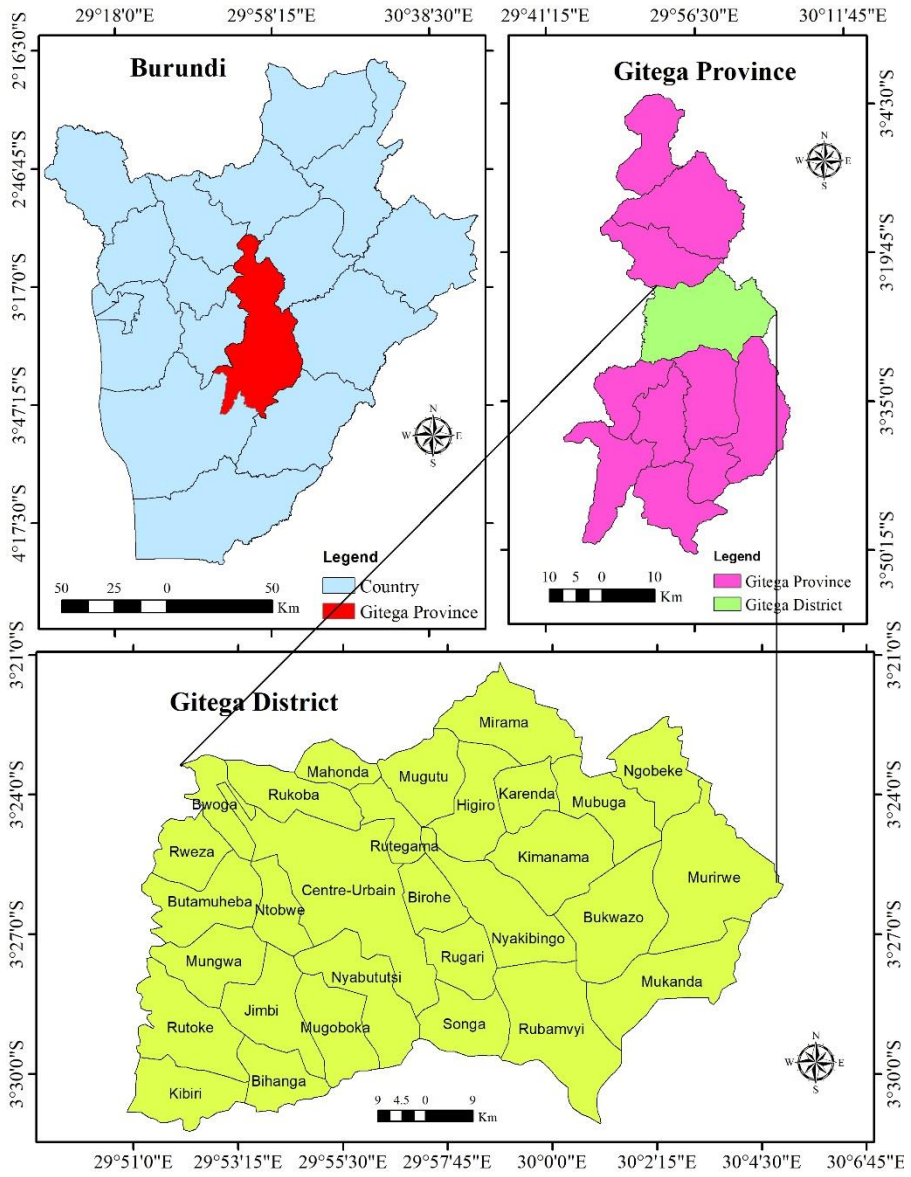

Figure 2. Location map of the study area

Table 1. Details of Landsat data

Satellite sensor	Path/row	Acquisition date	Bands	Resolution
Landsat 5 TM	172/062	20 June 1984	2, 3, 4	30 m
Landsat 7 ETM	172/062	17 August 2002	2, 3, 4	30 m
Landsat 8 OLI	172/062	23 July 2019	3, 4, 5	30 m

Prior to classifying the above satellite images from different dates, an image-based atmospheric correction was performed by subtracting a common minimum digital number (DN) value from the image using Idrisi software. Aside from noise removal, another image preprocessing based on image optical properties, such as sun elevation, angle, and spectral was applied using image metadata file. False-color composite and contrast stretching techniques were further applied to improve brightness and tonal differentiation between various features (Song et al., 2001).

2.2.1 Image classification and mapping

Several classification methods were developed to extract useful information from imagery. Two of the most popular land cover classification machines were also used in this research (Pulighe et al., 2016; Tilahun and Islam, 2015):

Supervised classification, which involves manually defining land cover classes and forcing signatures based on field identification and local knowledge of land cover types (Eastman, 2009; Patil et al., 2012). In this process, the common classification scheme in the LULC system (Anderson, 1976) and field survey data were used to form five LULC categories, for what training sits" samples were created.

Maximum Likelihood classifier was then used, whose function is to assign the pixel to the class with the highest probability. The training site samples generated during the supervised process were fully distributed on the entire image in terms of spectral information for each LULC class. The signature file containing spectral information was thereby generated (Eastman, 2009; Patil et al., 2012). Finally, ArcGIS software was used to map the five LULC categories: Agriculture, Built Area, Grass Land, Shrub Land, and Tree Cover. Figure 3 shows LULC maps for 1984, 2002, and 2019, respectively, and results of image classification and the area distribution is given in Table 2.

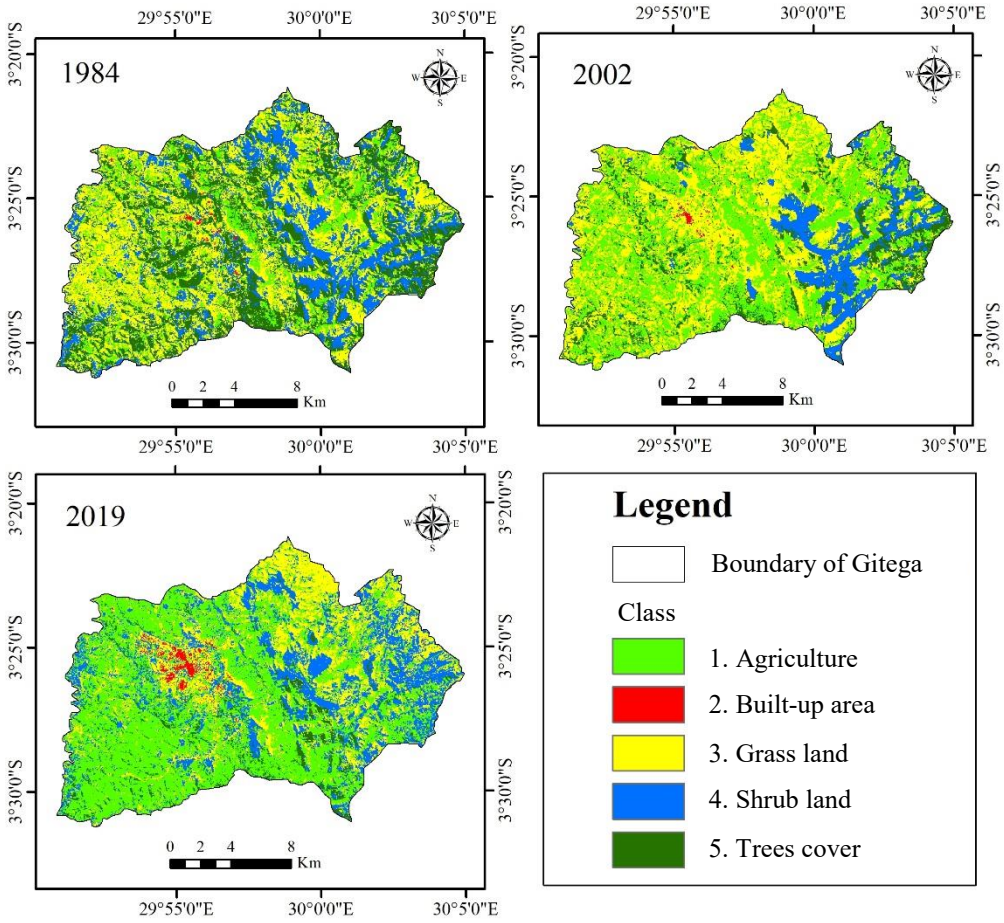

Figure 3. LULC maps from image classification for the year 1984, 2002, and 2019

Table 2. Area distribution for LULC in km^2

LULC class	1984	2002	2019
Agriculture	48	111.5	142
Built-up area	1	1.5	3
Grass land	112	121	73
Shrub land	61	31	66.5
Trees cover	81	38	18.5

2.2.2 Classification evaluation process

The high-resolution contemporary satellite imagery available on Google Earth pro was used to collect the ground truth data for 1984, 2002, and 2019 maps. Thirty pixels were selected using a stratified sample random method with ArcGIS to examine image classification accuracy (Pulighe et al., 2016; Tilahun and Islam, 2015). The confusion matrix

method reporting overall accuracy (OA) user's accuracy (UA), producer's accuracy (PA) and Kappa statistics (K) were generated (Dewan and Yamaguchi, 2009; Rwanga and Ndambuki, 2017). OA measures the percentage of total classified pixels that were truly labeled into the specific land cover and is computed by dividing the total correctly classified pixels (TCS or the sum of the diagonals) by the number of reference pixels (TS) in the error matrix using equations (1), (2), and (3):

$$OA = \frac{\Sigma TCS_{ij}}{TS} \quad (1)$$

$$PA = \frac{\Sigma TCS_{ij}}{TSc_i} \quad (2)$$

$$UA = \frac{\Sigma TCS_{ij}}{TSr_i} \quad (3)$$

Where; TCS_{ij} is the total number of the correctly classified pixels in row i and column j, TS is the total reference sample, TSc_j is the total number of pixels in column j and TSr_i is the total number of pixels in the row i. The quantitative measure of the level of agreement was done with utilization of kappa statistic (K) assumed that a K of 1 indicates ideal agreement, whereas a kappa of 0 indicates agreement equivalent to chance to truly classify the pixels as computed in the equation (4):

$$k = \frac{(TS \times TCS) - \Sigma\, TSc_j\, TSr_i}{TS^2 - \Sigma(TSc_j - TSr_i)} \quad (4)$$

Where; TCS_{ij} is the total number of the correctly classified pixels in row i and column j, TS is the total reference sample, TSc_j is the total number of pixels in column j and TSr_i is the total number of pixels in the row i. Moderate agreement of more than 85% and 82% for overall accuracy and Kappa statistics respectively was obtained as presented in Table 3.

Table 3. Results from classification accuracy assessment

Year	1984		2002		2019	
LULC	Producer	User	Producer	User	Producer	User
Agriculture	71	100	87	87	100	100
Built-up area	100	100	100	100	100	80
Grass land	100	62	82	62	100	88
Shrub land	71	83	66	100	66	100
Trees cover	100	100	100	100	100	100
Overall accuracy	86		86		93	
Kappa statistics	0.83		0.83		0.91	

2.3 Cellular Automata and Markov Chain for simulation the future LULC Change

The combination of Cellular Automata and Markov Chain models have been the most popular integrated model used for modelling spatial and temporal changes (Borana and Yadav, 2017; Sang et al., 2011). Markov Chain is a dynamic process that calculates the probability of changes from a particular object (e.g., vegetation) to another object (e.g., agriculture) in the next state depending on the former state. It has been used equally in LULC studies due to its ability to quantify conversion rates between two categories (Ghosh et al., 2017). Cellular Automata (CA) is a discrete dynamic system consisting of a normal finite cell network that can change in various directions in neighboring (Singh, 2003; Torrens, 2000). CA is also widely used in simulating LULC change because it is fairly close to GIS raster data (Pijanowski et al., 2002; Surabuddin et al., 2013). Therefore, the combination of the two above models was also applied in this study to simulate the LULC in 2019, 2038, and 2057 using the following equations (5) and (6) (Mondal et al., 2016; Nadoushan et al., 2015):

$$S(t, t+1) = Pij \times S(t) \quad (5)$$

Where; S (t) is the system status at time t; S (t+1) is the system status at a time of t+1, and Pij is the transition probability obtained in equation (6) below:

$$P = |P_{ij}| = \begin{vmatrix} P_{1,1} P_{1,2} \dots P_{1,N} \\ P_{2,1} P_{2,2} \dots P_{2,N} \\ \dots\dots\dots \\ P_{N,1} P_{N,2} \dots P_{N,N} \end{vmatrix} \quad 0 \le P_{ij} \le 1 \quad (6)$$

Where; P=Transition probability; Pij=stands for probability of changing from particular state i to another state j; P_N=state probability of any time, and N=Land cover type (Eastman, 2009; Mishra et al., 2014).

In this study, 1984, 2002, 2019 LULC maps were used to run Markov Chain. Firstly, 1984 and 2002 LULC maps were used as earlier and later images to project the 2019 LULC map (Figure 7), along with transition probability matrix shown in Table 4. This method produced a suitability map matching the current rate and quantity of 2019 LULC which will be further used to simulate future scenarios (Sang et al., 2011). The 1984 LULC map was used in CA-Markov as base map and Cellular automata iterations were set to 35 as the time interval between 1984 and 2019 to predict the 2019 LUC map. This simulation outcome was compared with the existing LULC to evaluate the model performance (Figure 4) (Gupta and Sharma, 2020). The 2019 LULC simulation was achieved using 1984-2002 transition probability area matrix, transition suitability map, and a set window technique 5*5 kernels called standard contiguous filter for influencing each cell center. After successful validation of 2019 simulation result, predictions of 2038 and 2057 LULC maps were done (Figure 7). At this stage, we used the 2019 real LULC map as the simulation's input, along with the relevant transition probability area matrices, and transitional suitability maps generated from Markov Chain (Nadoushan et al., 2015; Singh, 2003). Based on the modelling theory, we kept a default set of 5*5 kernel size contiguity filter, while the cellular automata iteration was set to 19 to simulate the 2038 LULC map, and the same method was used to simulate 2057 LULC map.

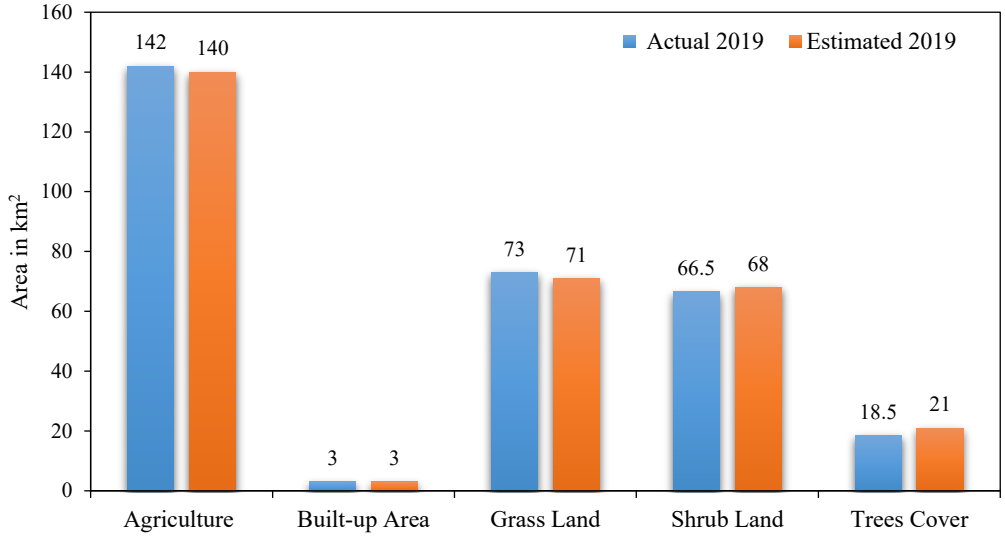

Figure 4. Area (in km^2) of LULC category in actual and simulated maps (2019)

2.4 Simulation accuracy and model evaluation

Simulation accuracy and model validation were determined by comparing the predicted LULC maps for 2019, 2038, and 2057 to the actual LULC map for 2019. The Kappa statistics is the most widespread method agreed to quantify the power and suitability of the simulation model (Maingi et al., 2002). This study utilized the submodule in Idrisi namely, GIS Analysis, to generate the Kappa index of Agreement shown in Table 5. The validation was done based on the assumption that the higher the kappa values, the better the model (Borana and Yadav, 2017). All kappa index values surpass the minimum acceptable standard and they range from 65% to 89%. This indicates a high degree of agreement between projected and actual LULC maps, thus a successful validation of the CA-Markov Chain model (Kundel and Polansky, 2003; van Vliet et al., 2011).

3. RESULTS AND DISCUSSION

3.1 LULC Change Analysis

The LULC changes analysis enables an understanding of physical modification or loss of features in the natural landscape such as vegetation and forests clearing, agricultural land, waterbody as worthwhile information useful for planning land use and environmental conservation (Wang et al., 2021). We applied the comparative method to analyze five LULC classes from image classifications based on remote sensing techniques (Dewan and Yamaguchi, 2009). The land use and land cover change analysis were accomplished by using land cover data with an interval of 35 years, from 1984 to 2019 which depicts

two sub-time intervals: 18 years (from 1984 to 2002), and 17 years (from 2002 to 2019).

Based on Figure 5, it is revealed that the landscape of Gitega in 1984 was extensively covered by Grass Land and Trees Cover: 112 km^2 (36.97%) and 81 km^2 (26.73%), respectively. Shrub Land is the third most dominant class, accounting for 61 km^2 (20.13%), while Agriculture and Built-up Area account for 48 km^2 (15.84%) and 1 km^2 (0.33%), respectively. In the year 2002, the study area was largely covered with Grass Land and Agriculture:121 km^2 (39.84%) and 111.5 km^2(36.92%), respectively. However, Trees Cover and Shrub Land decreased to 38 km^2 (12.24%) and 31 km^2 (10.21%), respectively, and Built-up Area had slightly increased. In 2019, the largest land cover was Agriculture with 142 km^2, an increase of 10% from 2002 to 2019. Grass Land took a second areal position with 73 km^2 due to a decrease of nearly 5%. Shrub Land rose to the third position due to an increase by 11.74% with an area of 66,5 km^2, while Trees Cover steeply decreased by 6.44% and occupied 18.5 km^2. Built-up Area has a steady increase of 1.5 km^2 from 2002-2019.

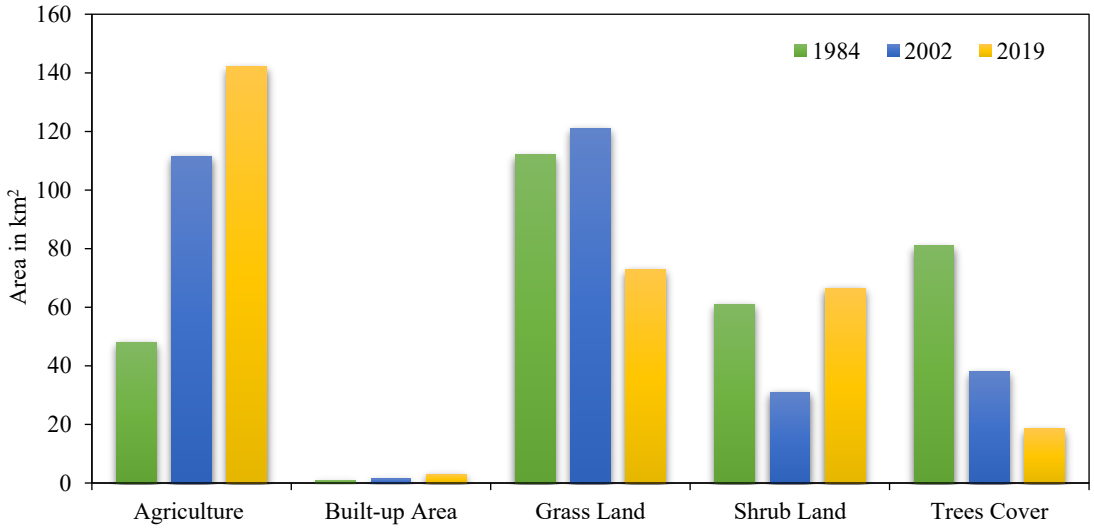

Figure 5. Comparison of existing LULC category by statistical area in km^2

Over past 35 years, the dynamic in LULC change patterns is intensely high. Trees Covers and Grass Land were continuously reduced by 62.5 km^2 at an annual rate of 1.79 km^2 and 39 km^2 at the rate of 1.12 km^2 per year, respectively. In contrast, a net change indicates a large extension in Agriculture of 94 km^2 at the rate of 2.68 km^2 per year. A slight increase is also detected in both Shrub Land and Built Area, which is 5.5 km^2 with a rate of 0.15, and 2 km^2 with a rate of 0.8 km^2 per year, respectively. For getting a better understanding, LULC change detection was investigated using Land Change Modeler (LCM), and the model outputs shown in Figure 6 are consistent with certain results of land cover change detection obtained using the same model. For instance, Gupta and Sharma (2020) have acknowledged interesting results of LULC change monitoring by LCM model in LULC dynamics study (over past 50 years) conducted in India. These decreasing areas in Trees Cover and Grass Land (by about 101.5 km^2 in total with an annual rate of 2.9 km^2) have been converted mostly into Agriculture (94 km^2), and little to Shrub Land and Built-up Area (7.5 km^2 together) from 1984 to 2019.

Similar trends of LULC change, especially deforestation and agricultural expansion, were globally addressed (FAO, 2016), and in many other developing countries (Alawamy et al., 2020; Berakhi, 2013; Henry et al., 2011; Islam et al., 2018). Interesting LULC change issues in terms of urban sprawl were recently dealt with by Patel et al. (2019) in India. Thereby, a general perception is that forest and vegetation reductions lead to dramatic degradation of productive ecosystems and loss of biodiversity (Wang et al., 2021). Primarily, the land degradation will radiate outwards within the global environment (IPCC, 2019; Marathianou et al., 2000; Niyogi et al., 2009). Deforestation alters hydrological processes and affects water conductivity like surface runoff (El-Hassanin et al., 1993) and, therefore, the occurrence of soil erosions and soil losses as observed in the study area (Henry et al., 2011; Nijimbere et al., 2019; Niyuhire, 2018; Nzabakenga et al., 2013).

A review of the trends in population growth and density (476 people/km^2) in the Gitega District can reveal that the most LULC changes are likely the shortcomings of human encroachment on natural land resources and ecosystems (Kamungi et al., 2005). In this study, the results of the LULC change analysis for the last thirty-five years were used to make predictions for the next thirty-eight years.

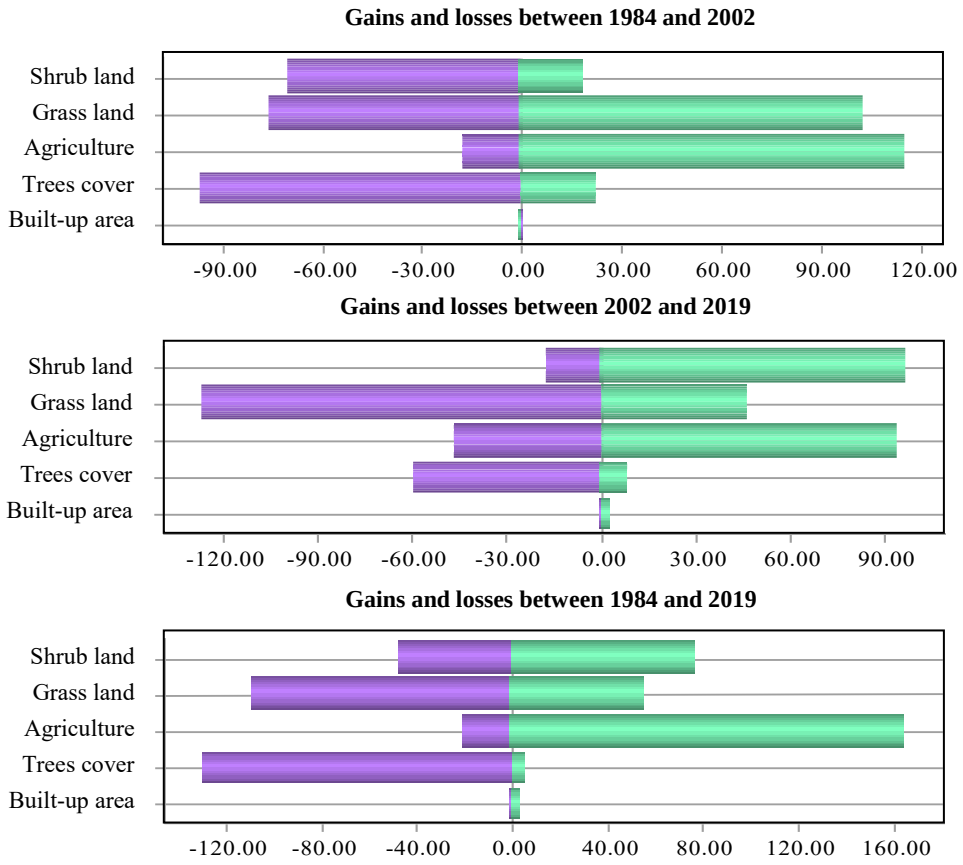

Figure 6. Gains (Green) and losses (Purple) in km^2 by category of LULC in different periods

3.2 Simulation result analysis

CA-Markov Chain simulation model requires earlier and later LULC maps to predict the future scenario (Sang et al., 2011). Future LULC simulations were projected for 2057 with a time interval of 38 years, from 2019 to 2057, which also depict two sub-time intervals: 19 years (from 2019 to 2038) and 19 years (from 2019 to 2057). According to the Markov Chain concept, changes that occurred in the previous period can be used to predict changes in the next period (Ghosh et al., 2017; Wang et al., 2021). In this study, the simulation inputs were the real and projected LULC maps for 2019 and the probability matrix for the transition to land-use change in 2019-2038 and 2019-2057.

Based on the theory of transition probability, the Markov model performs the likelihood of a change from one land cover category to another within a dimensioned matrix of LULC classes (Nadoushan et al., 2015). For example, the analysis of the results from Markov Chain application in this study given in the cross-tabulation showed revealed that from 2019 to 2038, the probability of change for Agriculture to Agriculture is 68.24%, while the probability of future change of Agriculture to Grass Land is 20.76%. Trees Cover has a probability as low as 5.9% to remain as they are but has a probability of 37.06% to change to Agriculture and the same process for other LULC classes. In the second prediction scenario, from 2019 to 2057, Agriculture has the highest probability of 71.09% to remain the same in 2057, whereas Trees Cover indicates the most declining probability of 3% to remain same in 2057. Built-up Area, Grass Land, and Shrub Land have the probability of 49.01%, 30.84%, and 26.24%, respectively, to remain as they are in 2019. Table 4 records the transition probability matrix of Gitega District LULC conversions that could occur from 2019 to 2038 and 2019 to 2057, with dimensions of 5×5.

Table 4. Transition probability matrices used during simulation process

a. Probability of changing from … by 2019 to:

1984	Agriculture	Built-up Area	Grass Land	Shrub Land	Trees Cover	Total	Omission
Agriculture	0.629	0.0072	0.1051	0.2336	0.0251	1	0.371
Built-up Area	0.1401	0.4638	0.198	0.1903	0.0078	1	0.802
Grass Land	0.3922	0.0186	0.4532	0.1131	0.0229	1	0.9814
Shrub Land	0.2925	0.0166	0.3138	0.3534	0.0237	1	0.6466
Trees Cover	0.4634	0.0071	0.1968	0.294	0.0387	1	0.9613
Total	1.9172	0.5133	1.2669	1.1844	0.1182	5	
Commission	1.2882	0.0495	0.8137	0.831	0.0795		

b. Probability of changing from … by 2038 to:

2019	Agriculture	Built-up Area	Grass Land	Shrub Land	Trees Cover	Total	Omission
Agriculture	0.6824	0.0045	0.2076	0.0839	0.0216	1	0.3176
Built-up Area	0.1681	0.4321	0.1959	0.1987	0.0052	1	0.8041
Grass Land	0.5423	0.0021	0.3811	0.0601	0.0144	1	0.9979
Shrub Land	0.368	0.0175	0.3905	0.2139	0.0101	1	0.7861
Trees Cover	0.3706	0.0039	0.2147	0.3518	0.059	1	0.941
Total	2.1314	0.4601	1.3898	0.9084	0.1103	5	
Commission	1.449	0.028	1.0087	0.6945	0.0513		

c. Probability of changing from…by 2057 to:

2019	Agriculture	Built-up Area	Grass Land	Shrub Land	Trees Cover	Total	Omission
Agriculture	0.7109	0.0027	0.1733	0.0901	0.023	1	0.2891
Built-up Area	0.1248	0.4901	0.2536	0.1256	0.0059	1	0.7464
Grass Land	0.4026	0.0034	0.3084	0.2591	0.0265	1	0.9966
Shrub Land	0.4801	0.0083	0.2102	0.2648	0.0366	1	0.7352
Trees Cover	0.6446	0.004	0.1124	0.2032	0.0358	1	0.9642
Total	2.363	0.5085	1.0579	0.9428	0.1278	5	
Commission	1.6521	0.0184	0.7495	0.678	0.092		

Cellular Automata and Markov Chain models were spatially integrated to predict change location (Verburg, 2006). This simulation process for 2019-2057, which combines Cellular Automata and the Markov model, is similar to the simulation process for 1984-2019. The difference was in the time interval of input data used as the basis for simulation, which was due to the need for high-quality image data to successfully detect and model Gitega District LULC changes. The transition probability and changing area prediction from the Markov Chain process served as the input basis for Cellular Automata to determine the change location represented in pixel (Nadoushan et al., 2015; Singh, 2003). The simulation results are presented as predicted LULC maps. Table 5 displays the index values that indicate reasonable agreement for the model validation and the prediction results accuracy.

Table 5. Simulation accuracy assessment result by kappa index

k indicators	2019	2038	2057
K_{no}	0.7205	0.8330	0.7870
$K_{location}$	0.7569	0.8785	0.8324
$K_{location\ Strata}$	0.7569	0.8785	0.8324
$K_{standard}$	0.6565	0.7978	0.7528

The Figure 7 depicts maps of LULC prediction results in the Gitega District for 2038 and 2057 respectively simulated using estimated LULC map for 2019.

Based on Table 6, it is projected that Agriculture will continuously expand with the increase of 14 km^2 and 30 km^2 in 2038 and 2057, respectively. Built-up Area will increase by 6 km^2 in 2057. However, trees cover, grass land, and shrub land will be decreasing by 11.5 km^2, 13 km^2 and 11.5 km^2,

respectively, in 2057. These predicted trends of LULC change showing such continuous agricultural expansion at expenses of forest and vegetation are also similar to those reported by other LULC modelling studies (Henry et al., 2011; Mondal et al., 2016; Nadoushan et al., 2015; Wang et al., 2021). Eventually, a better decision is needed to avoid these projected major LULC changes in Gitega District. Table 6 displays the results of change analysis of predicted LULC maps.

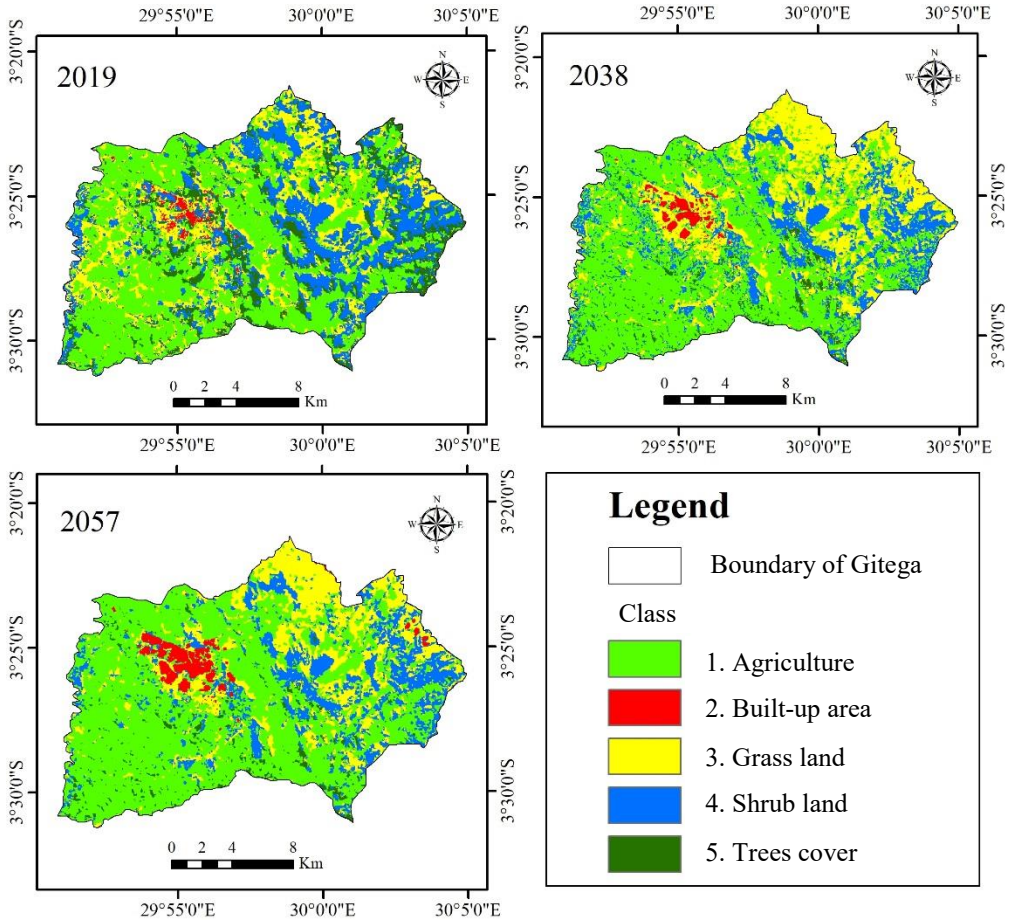

Figure 7. Predicted LULC maps for 2019, 2038, and 2057

Table 6. Change analysis of future projected LULC

LULC category	Simulated area (in km^2)		Change detection (in km^2)	
	2038	2057	2038-2019	2057-2019
Agriculture	156	172	14	30
Built-up area	5	9	2	6
Grass land	78	60	5	-13
Shrub land	54	55	-12.5	-11.5
Trees cover	10	7	-8.5	-11.5

4. CONCLUSION

This paper assessed the rate and trends of change in LULC patterns quantified and predicted using Geoinformatics in Gitega District. The Change analysis was performed using 5 LULC classes obtained from images classification of years 1984, 2002, and 2019 and was highlighted with Land Change Modeler. Markov Chain and CA-Markov models were applied to project future trends of LULC changes in 2038 and 2057. Satisfactory accuracy with good agreements of more than 85% and 82%, respectively, for overall accuracy and Kappa statistics was achieved. RS, GIS, and Cellular Automata and Markov Chain models were therefore proven to be

effective tools for LULC change monitoring and generating multi-temporary land cover dataset to assist decision-makers towards land use planning and environmental protection.

Overall findings reveal dramatic decreasing area in Trees Cover and Grass Land of 101.5 km^2 together, and which was likely converted mostly to Agriculture (which increased by 94 km^2 at a rate of 2.68 km^2 per year), and to Shrub Land and Built-up Area (7.5 km^2 together) over the past 35 years. These results are reflective of the current rate, trends, and magnitude of LULC changes and local policies in the study area. If Gitega attempts to avoid further irreversible land degradation and associated environmental problems, the government and policymakers should urgently apply agroecological approaches and reforestation.

Similar trends in LULC change patterns are revealed by predictive result analysis. Agriculture has 71.09% probability of remaining as Agriculture in 2057, with an expected area of 172 km^2 (56.76%). On the other hand, Trees Cover have the lowest probability of 3% to remain as Trees in 2057, with an area of 7 km^2. These study outcomes are the potential to support decision-making to undertake restoration measures of land degradation and future sustainable land use management and environmental presser-vation . However, future studies should consider the correlation of Gross Domestic Products (GDP) and Population Growth with these LULC changes analysis results.

ACKNOWLEDGEMENTS

I would like to thank Thailand International Cooperation Agency and Naresuan University for their financial and material support of this research. I am also grateful to the Burundian government and the local community for supplying useful data for this study. Anonymous reviewers and editors are also acknowledged for constructive comments.

REFERENCES

Alawamy JS, Balasundram SK, Hanif AHM, Sung CTB. Detecting and analyzing land use and land cover changes in the region of Al-Jabal Al-Akhdar, Libya using time-series landsat data from 1985 to 2017. Sustainability 2020;12(11):4490.

Anderson JR. A Land Use and Land Cover Classification System for Use with Remote Sensor Data. US Government Printing Office; 1976.

Bai ZG, Dent DL, Olsson L, Schaepman ME. Proxy global assessment of land degradation. Soil Use and Management 2008;24(3):223-34.

Baker WL. A review of models of landscape change. Landscape Ecology 1989;2(2):111-33.

Berakhi RO. Implication of Human Activities on Land Use Land Cover Dynamics in Kagera Catchment, East Africa [dissertation]. Southern Illinois University Carbondale; 2013.

Boissière M, Sheil D, Basuki I, Wan M, Le H. Can engaging local people's interests reduce forest degradation in Central Vietnam? Biodiversity and Conservation 2009;18(10): 2743-57.

Borana S, Yadav S. Comparison of model validation techniques for land cover dynamics in Jodhpur City. International Journal of Emerging Trends and Technology in Computer Science. 2017;6(5):215-9.

Burrell AL, Evans JP, Liu Y. The impact of dataset selection on land degradation assessment. Journal of Photogrammetry and Remote Sensing 2018;146:22-37.

Dewan AM, Yamaguchi Y. Using remote sensing and GIS to detect and monitor land use and land cover change in Dhaka Metropolitan of Bangladesh during 1960-2005. Environmental Monitoring and Assessment 2009;150(1-4):237.

Eastman JR. Idrisi Taiga guide to GIS and image processing [Internet]. 2009 [cited 2020 Oct 15]. Available from: http://web.pdx.edu/~nauna/resources/TaigaManual.pdf.

El-Hassanin A, Labib T, Gaber E. Effect of vegetation cover and land slope on runoff and soil losses from the watersheds of Burundi. Agriculture, Ecosystems and Environment 1993;43(3-4):301-8.

Food and Agriculture Organization (FAO). State of the world's forests, 2016: Forests and agriculture: Land use challenges and opportunities [Internet]. 2016 [cited 2021 Mar 7]. Available from: http://www.fao.org/3/a-i5588e.pdf.

Ghosh P, Mukhopadhyay A, Chanda A, Mondal P, Akhand A, Mukherjee S, et al. Application of cellular automata and markov-chain model in geospatial environmental modeling: A review. Remote Sensing Applications: Society and Environment 2017;5:64-77.

Gómez C, White JC, Wulder MA. Optical remotely sensed time series data for land cover classification: A review. ISPRS Journal of Photogrammetry and Remote Sensing. 2016; 116:55-72.

Guichaoua A. Population migrante et types de mobilité au Burundi. Les Cahiers d'Outre-Mer 1982;35(138):141-59 (in French).

Gupta R, Sharma LK. Efficacy of spatial land change modeler as a forecasting indicator for anthropogenic change dynamics over five decades: A case study of Shoolpaneshwar Wildlife Sanctuary, Gujarat, India. Ecological Indicators 2020;112:106171.

Halmy MWA, Gessler PE, Hicke JA, Salem BB. Land use/land cover change detection and prediction in the north-western coastal desert of Egypt using markov-CA. Applied Geography 2015;63:101-12.

Henry M, Maniatis D, Gitz V, Huberman D, Valentini R. Implementation of REDD+ in sub-Saharan Africa: State of knowledge, challenges and opportunities. Environment and Development Economics 2011;16(4):381-404.

Intergovernmental Science-Policy Platform on Biodiversity and Ecosystem Services (IPBES). Summary for policymakers of the assessment report on land degradation and restoration [Internet]. 2018 [cited 2021 Mar 10]. Available from: https://www.ipbes.net/system/tdf/spm_3bi_ldr_digital.pdf?file=1&type=node&id=28335.

Intergovernmental Panel on Climate Change (IPCC). Climate Change and Land: An IPCC Special Report on Climate Change, Desertification, Land Degradation, Sustainable Land Management, Food Security, and Greenhouse Gas Fluxes in Terrestrial Ecosystems. IPCC; 2019.

Islam K, Jashimuddin M, Nath B, Nath TK. Land use classification and change detection by using multi-temporal remotely sensed imagery: The case of Chunati wildlife sanctuary, Bangladesh. The Egyptian Journal of Remote Sensing and Space Science 2018;21(1):37-47.

Kamungi PM, Oketch JS, Huggins C. Land access and the return and resettlement of IDPs and refugees in Burundi: From the Ground Up. Project Relationships between Land Rights, Conflict and Peace in Sub-Sahara Africa. Pretoria: Institute for Security Studies; 2005 p. 195-267.

Kumar M, Mukherjee N, Sharma GP, Raghubanshi A. Land use patterns and urbanization in the holy city of Varanasi, India: A scenario. Environmental Monitoring and Assessment 2010;167(1):417-22.

Kundel HL, Polansky M. Measurement of observer agreement. Radiology 2003;228(2):303-8.

Lambin EF, Rounsevell MD, Geist HJ. Are agricultural land-use models able to predict changes in land-use intensity? Agriculture, Ecosystems and Environment 2000;82(1-3): 321-31.

Liu Q, Shi T. Spatiotemporal differentiation and the factors of ecological vulnerability in the Toutun River Basin based on remote sensing data. Sustainability 2019;11(15):4160.

Maingi J, Kepner S, Edmonds W. Accuracy assessment of 1992 landsat-MSS derived land cover for the Upper San Pedro Watershed (US/Mexico). Las Vegas: Environmental Protection Agency; 2002.

Marathianou M, Kosmas C, Gerontidis S, Detsis V. Land-use evolution and degradation in Lesvos (Greece): A historical approach. Land Degradation and Development 2000; 11(1):63-73.

Meyer WB, Turner BL. Changes in Land Use and Land Cover: A Global Perspective. United Kingdom: Cambridge University Press; 1994.

Mishra VN, Rai PK, Mohan K. Prediction of land use changes based on land change modeler (LCM) using remote sensing: A case study of Muzaffarpur (Bihar), India. Journal of the Geographical Institute Jovan Cvijic SASA 2014;64(1):111-27.

Mondal MS, Sharma N, Garg P, Kappas M. Statistical independence test and validation of CA markov land use land cover (LULC) prediction results. The Egyptian Journal of Remote Sensing and Space Science 2016;19(2):259-72.

Moore ML. An Examination of Contributing Factors to Land Use/Land Cover Change in Southern Belize and the Use of Satellite Image Analysis to Track Changes [dissertation]. Ames, Iowa State University; 2007.

Nadoushan MA, Soffianian A, Alebrahim A. Modeling land use/cover changes by the combination of markov chain and cellular automata markov (CA-Markov) models. Journal of Earth, Environment and Health Sciences 2015;1(1):16.

Ndzabandzaba C. Data Sharing for Sustainable Development in Less Developed and Developing Countries. Global Sustainable Development Report; 2015.

Nijimbere G, Lizana CR, Riveros PJIK. Assessment of soil erosion of Burundi using remote sensing and GIS by RUSLE model. RUDN Journal of Ecology and Life Safety 2019;27(1):17-28.

Niyogi D, Mahmood R, Adegoke JO. Land-use/land-cover change and its impacts on weather and climate. Boundary Layer Meteorology 2009;133(3):297.

Niyuhire MC. Integrated Soil Fertility Management for Bean-Maize Based Farming Systems in Gitega Province, Burundi: Understanding and Enhancing the Agronomic and Economic Benefits of Organic and Mineral Inputs [dissertation]. Belgium, KU Leuven; 2018.

Nzabakenga A, Feng LX, Yaqin H. Agricultural income determinants among smallholder farmers: Case of northern part of Burundi. Asian Journal of Agriculture and Rural Development 2013;3(11):780-7.

Patel SK, Verma P, Singh GS. Agricultural growth and land use land cover change in peri-urban India. Environmental Monitoring and Assessment 2019;191(9):1-17.

Patil MB, Desai CG, Umrikar BN. Image classification tool for land use/land cover analysis: A comparative study of maximum likelihood and minimum distance method. International Journal of Geology, Earth and Environmental Sciences 2012;2(3):189-96.

Pijanowski BC, Brown DG, Shellito BA, Manik GA. Using neural networks and GIS to forecast land use changes: A land transformation model. Computers, Environment and Urban Systems 2002;26(6):553-75.

Poursanidis D, Chrysoulakis N, Mitraka Z. Landsat 8 vs. Landsat 5: A comparison based on urban and peri-urban land cover mapping. International Journal of Applied Earth Observation and Geoinformation 2015;35:259-69.

Pulighe G, Baiocchi V, Lupia F. Horizontal accuracy assessment of very high resolution google earth images in the city of Rome, Italy. International Journal of Digital Earth 2016;9(4):342-62.

Rwanga SS, Ndambuki JM. Accuracy assessment of land use/land cover classification using remote sensing and GIS. International Journal of Geosciences 2017;8(04):611.

Sang L, Zhang C, Yang J, Zhu D, Yun W. Simulation of land use spatial pattern of towns and villages based on CA-markov model. Mathematical and Computer Modelling 2011;54(3-4):938-43.

Serneels S, Lambin EF. Proximate causes of land-use change in Narok District, Kenya: A spatial statistical model. Agriculture, Ecosystems an Environment 2001;85(1-3):65-81.

Shen L. Multi-Layer Perceptron-Markov Chain Based Geospatial Analysis of Land Use and Land Cover Change: A Case Study of Stoney Creek Watershed, BC, Canada [dissertation]. China, North China Electric Power University; 2019.

Singh AK. Modelling Land Use Land Cover Changes Using Cellular Automata in a Geo-Spatial Environment [dissertation]. Netherlands, ITC; 2003.

Song C, Woodcock CE, Seto KC, Lenney MP, Macomber SA. Classification and change detection using Landsat TM data: When and how to correct atmospheric effects? Remote Sensing of Environment 2001;75(2):230-44.

Surabuddin M, Sharma N, Kappas M, Garg P. Modeling of spatio-temporal dynamics of land use and land cover in a part of Brahmaputra River basin using Geoinformatic techniques. Geocarto International 2013;28(7):632-56.

Tilahun A, Islam Z. Google earth for land use land cover change detection in the case of Gish Abbay Sekela, West Gojjam, Amhara state, Ethiopia. International Journal of Society and Humanities 2015;3:80-7.

Torrens PM. How Cellular Models of Urban Systems Work (1. Theory). Centre for Advanced Spatial Analysis, UK: University College London; 2000.

Turner BL, Lambin EF, Reenberg A. The emergence of land change science for global environmental change and sustainability. Proceedings of the National Academy of Sciences 2007;104(52):20666-71.

Twisa S, Buchroithner MF. Land use and land cover change detection in Wami River Basin, Tanzania. Land 2019; 8(9):136.

United Nations Data Retrieval System (UNdata). A world of information [Internet]. 2020 [cited 2021 Mar 5]. Available from: https://data.un.org/en/iso/bi.html.

van Vliet J, Bregt AK, Hagen-Zanker A. Revisiting kappa to account for change in the accuracy assessment of land use change models. Ecological Modelling 2011;222(8):1367-75.

Vassolo S, Neukum C, Tiberghien C, Heckmann M, Hahne K, Baranyikwa D. Hydrogeology of a weathered fractured aquifer system near Gitega, Burundi. Hydrogeology Journal 2019;27(2):625-37.

Verburg PH. Simulating feedbacks in land use and land cover change models. Landscape Ecology 2006;21(8):1171-83.

Verma P, Raghubanshi A. Rural development and land use land cover change in a rapidly developing agrarian South Asian landscape. Remote Sensing Applications: Society and Environment 2019;14:138-47.

Vila JPS, Barbosa P. Post-fire vegetation regrowth detection in the Deiva Marina region (Liguria-Italy) using landsat TM and ETM+ data. Ecological Modelling. 2010;221(1):75-84.

Wang SW, Munkhnasan L, Lee WK. Land use and land cover change detection and prediction in Bhutan's high altitude city of Thimphu, using cellular automata and markov chain. Environmental Challenges 2021;2:100017.